Generalized Line Integral Convolution Rendering of Diffusion Tensor Fields

Edward HSU[1]
[1]Duke University, Department of Biomedical Engineering, Durham, NC USA;

INTRODUCTION

Due to the multi-dimensionality of the data, visualization of diffusion tensor fields, hence tissue microstructures, has generally required a tradeoff between the information included and spatial resolution of the representation. For example, although object-based renderings (e.g., ellipsoids [1]) can simultaneously depict the diffusivities and orientations of all principal diffusion axes, spatial resolution and continuity are sacrificed to avoid visual cluttering. In contrast, pixel value-based representations (e.g., falsecolor-coded fiber angles [2]) circumvent these spatial issues, but only partial information regarding diffusion anisotropy is shown each time, and the viewer often needs to be re-trained to correctly interpret the coding schemes.

In this study, we applied a line-integral convolution (LIC) technique [3] to visualize diffusion tensor fields obtained via DTI [4]. Special considerations were incorporated to extend the original 2D method for rendering 3D diffusion tensor fields, and to reconstruct both the principal and second-order anisotropy of water diffusion. The generalized LIC technique is demonstrated in reconstructing myocardial fiber and lamellar architectures. Results indicate the approach to be robust, scalable, and share key advantages of both object- and pixel value-based means to visualize tissue microstructure.

METHODS

The previously described LIC algorithm [3] was extended to perform constrained propagation of pixels of a 3D input texture field $T(x, y, z)$ subject to the local directional field $V(x, y, z) = (v_x, v_y, v_z)$, and consisted of two steps: streamline calculation and contour integration. For the pixel located at (x, y, z), the streamline starts at the center of the pixel $P_0 = (sx_0, sy_0, sz_0) = (x+0.5, y+0.5, z+0.5)$. Because eigenvectors have unit length, the distance to the nearest pixel cell border Δs_i (i = 1, 2, 3,...) is the minimum of the set

$$\{(\text{ceil}[sx_{i-1}]-sx_{i-1})/v_x, (\text{ceil}[sy_{i-1}]-sy_{i-1})/v_y, (\text{ceil}[sz_{i-1}]-sz_{i-1})/v_z\}.$$

Moreover, the next point on the streamline is given by

$$P_i = P_{i-1} + \Delta s_i \cdot V(\text{floor}[P_{i-1}]).$$

The procedures are iterated until a desired length $L = \Sigma_i \Delta s_i$ is reached. To visualize the bi-directional anisotropic process, the "backward" streamline points, denoted by P_j, are computed similarly using the reversed eigenvector $V'(x, y, z) = -V(x, y, z)$.

The contour integration step calculates the pixel intensity of the output image $I(x, y, z)$ based on the weighted sum of the input texture field along the streamline,

$$I(x, y, z) = (\Sigma_i T(\text{floor}[P_i]) \cdot h_i + \Sigma_j T(\text{floor}[P_j]) \cdot h_j)/(\Sigma_i h_i + \Sigma_j h_j),$$

where the incremental weighting factor h_i (or h_j) is given by $h_i = \int_{\Delta s i} w(s)ds;$. In the present case, $w(s)$ is set identically to unity, and h_i is thus equal to the segmental length of Δs_i.

The generalized LIC algorithm was demonstrated by reconstructing the myocardial architecture of an intact, excised, and formalin-fixed canine heart obtained by reduced-encoding DTI [5] (256 x 256 x 256 matrix size, 10 cm FOV). To reconstruct both myocardial fiber and lamellar structures, two passes of the LIC reconstruction were performed. First, a salt-and-pepper input texture field (20% filling density) was created by a random number generator, and using the principal diffusion tensor eigenvectors as the directional field, an intermediate output was reconstructed via LIC ($L = 40$). The output corresponds to axisymmetric, fiber-only rendering of the myocardial architecture. Moreover, to reconstruct the myocardial lamellar structure, the intermediate output field was in turn used as the input texture field, with the secondary diffusion tensor eigenvectors as the directional field, in LIC (with a shorter integration length, $L = 8$) to yield the final output. The salt-and-pepper texture density and the integration lengths of the two LIC passes were selected empirically for optimal visualization effect. Finally, the output field, essentially a 3D volume array, was viewed using a conventional slice viewer, and also volume-rendered for 3D realism.

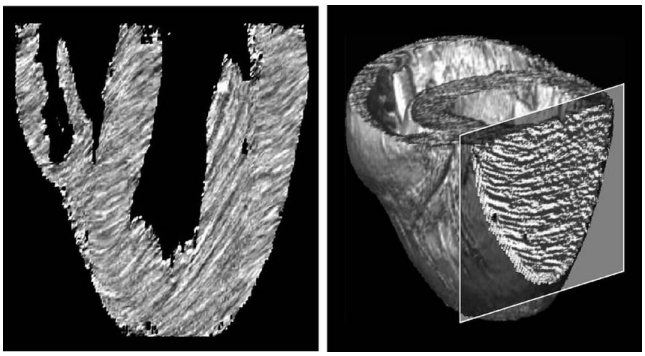

Fig 1. Generalized LIC rendering of myocardial architecture.

RESULTS

Figure 1 shows the results of generalized LIC reconstruction of myocardial architecture, including a middle long-axis slice (left), and rendered 3D volume with long-axis cut-away (right) of the same heart. Details of the myocardial architecture are clearly discernable. Because two dimensions of diffusion anisotropy were incorporated in the rendering, the observed structural patterns correspond to a combination of the myocardial fiber and lamellar architectures.

DISCUSSION AND CONCLUSIONS

The results show that the LIC reconstruction share the key advantages of both object-based and pixel value-based renderings of diffusion tensor fields. As demonstrated, it can be used to reconstruct orientations of more than one principal axis of diffusion. Moreover, its pixel-based nature preserves the spatial resolution and segment-wise continuity of the reconstruction. Although the present demonstration is based on selected parameters of rendering, without loss of generality and depending on the specific application, the LIC reconstruction can be readily scaled by, for example, changing the input texture density, streamline lengths, and spatial resolution (e.g., via interpolation) to enhance visualization effect.

As with most visualization techniques, the LIC method can be computationally intensive. The computation time increases proportionally with the prescribed streamline lengths and each dimension of resolution increase. However, the streamline computation process in the original LIC implementation (and as outlined in the present study section) involves a high degree of redundancy (because many pixels are connected by the same or parallel streamlines), techniques exist [6] and can be incorporated to improve the reconstruction time efficiency.

In conclusion, we have shown that the generalized LIC technique is a robust tool for visualizing diffusion tensor fields and can be used to effectively reconstruct microstructures of tissues such as the myocardium.

References

[1] Pierpaoli C, et al. Radiology 1996; 201:637-648.
[2] Pajevic S, Pierpaoli C. Magn. Reson. Med. 1999; 42:526-540.
[3] Cabral B. Leedom C. Proc. SIGGRAPH 93, pp. 263-270.
[4] Basser PJ et al. Biophys J. 1994; 66:259-267.
[5] Davis B et al. Proc. BMES Annual Meeting, 2000; T4.41.
[6] Stalling D, Hege H.C. Proc SIGGRAPH 95, pp. 249-256.

Acknowledgments

Many thanks to K. Sampson, PJ Chiang and Mrs. E. Fitzsimons for their technical and editorial assistance. Supported by funds from AHA B98425N, and NIH/NCRR P41-RR05959.